Magnetic relaxation process determination in the Co/Au nanoparticle system

Pavol Hrubovčák [*]

Frank Laboratory of Neutron Physics, Joint Institute for Nuclear Research, Dubna 141980, Russia
and Department of Solid State Physics, P. J. Šafárik University, Park Angelinum 9, Košice, Slovakia

Adriana Zeleňáková

Department of Solid State Physics, P. J. Šafárik University, Park Angelinum 9, Košice, Slovakia

Vladimír Zeleňák

Department of Inorganic Chemistry, P. J. Šafárik University, Moyzesova 11, Košice, Slovakia

Davide Peddis and Dino Fiorani

ISM-CNR, Area della Ricerca Roma 1, Via Salaria km 29.300, Cassella Postale 10, 00016 Monterotondo, Italy

Nonequilibrium magnetic dynamics has been investigated in the Co/Au bimetallic nanoparticle system. The system exhibits typical superparamagnetic behavior at higher temperatures and unequivocal hallmarks of magnetic relaxation process at $T \sim 7$ K. Since different scenarios of magnetic transition can be hypothesized here, detailed analysis of magnetization ac and dc experimental data has been performed. Specific methods have been employed in order to reveal the nature of the examined process. The observation of critical dynamics [power-law divergence of the relaxation time at T_g; dynamic scaling of $\chi''(T, f)$ data] and aging effects in the presence of strong interparticle interactions provide evidence that the system undergoes a transition to a super-spin-glass state rather than to a super-spin-blocked state.

I. INTRODUCTION

The current introduction of nanotechnologies into various areas of human activities is facilitated by the progress that has been made in the investigation of the properties of nanomaterials. Many interesting phenomena characteristic of nanoscale structures have been revealed and described. Profound understanding of their origin is crucial for the development of tuned nanosytems with desired qualities. Consequently, advanced nanomaterials as the products of hi-tech engineering can easily find a multitude of their applications [1–3].

In the case of magnetic nanoparticles (NPs), size is the crucial parameter affecting their properties and behavior. In contrast with bulk or microstructures, fine magnetic NPs are characterized by the significantly enhanced surface-to-volume ratio. This results in the induction and promotion of peculiar surface effects [4]. The effects are predominantly triggered by the irregularities and atom vacancies in the crystal lattice, which causes spin canting in the surface layer [5,6] or even in the core of a particle [7,8]. One of the consequences of spin frustration may manifest itself in the onset of the spin-glass-like state. It has been documented in a variety of nanoparticle systems at sufficiently low temperatures [9,10]. In the case of larger magnetic NPs, the surface effects can be regarded as negligible. Atomic spins in the ferrromagnetic body of the particle align parallel. They behave like a giant unit, superspin, with the magnitude several orders higher than the magnitude of a single atom spin [11]. Since a number of experimental studies have revealed distinct behavior of magnetic NPs characterized by superspins from atomic spin systems, there is a demand for proper documentation and new descriptions of their specific properties. The first theory of magnetization processes in the system of monodomain ferromagnets was proposed by Stoner and Wolfarth in 1948 [12]. After 1 yr, Néel introduced his relaxation theory describing the temperature-dependent magnetization reversal in monodomain particles, and the theory of superparamagnetism was established [13]. However, the model does not assume mutual interparticle interactions. This turned out to be the main reason for its discrepancy with results of experimental investigation on highly concentrated magnetic nanoparticle systems in the past two decades [14–16]. On the contrary, a number of recent studies shows that, in the assembly of sufficiently concentrated magnetic nanoparticles, superspins are able to interact via dipole-dipole interaction. If the strength of the mutual interactions is high enough, superspins exhibit collective behavior, and the super-spin-glass state can be observed [17,18]. Its denotation comes from the similarity of its behavior to the atomic spin glass, although the origins of both states are completely different. Exchange and Ruderman-Kittel-Kasuya-Yosida interaction between atomic spins are assumed to be the main forces of the spin-glass formation [19]. On the other hand, the frustration of superspins below

[*]pavol.hrubovcak@upjs.sk

the super-spin-glass temperature T_{SSG} is facilitated by strong dipole-dipole interaction, random distribution of particles' easy axes, and short interparticle distance [18]. Under these specific conditions, a magnetic system is not in equilibrium and exhibits hallmarks typical of spin glasses. However, due to a tremendous variability among magnetic nanoparticle systems, not all of the spin-glass-like state signatures are always apparent. Even in the particular system, they can be smeared as a consequence of particle size and shape polydispersity, concentration inhomogenities, or other effects. Considerable effort of the scientific community that has been devoted to the investigation of the spin-glass state has led to the development of several methods suitable for the recognition of its behavior. Recently, some of these techniques have been successfully extended to the magnetic nanoparticle ensembles with strong interparticle interactions. The most relevant of them have been employed in our paper, and they are discussed later.

This paper presents an experimental study of a relaxation process and magnetic interactions in the bimetallic Co/Au (core/shell) nanoparticle system. When assuming structural characteristics of the examined Co/Au particles (regular spherical shapes, narrow size distribution), the system can be regarded as a typical representative of a magnetic core/shell nanoparticle ensemble. In contradiction with its clear superparamagnetic behavior at higher temperatures, signatures of strong interactions are observed in the low-temperature region. Hence, we report the application of appropriate methods for nonequilibrium magnetization dynamics characterization to the common core/shell nanoparticle system. Employing these techniques, we determined the presence, strength, and nature of mutual interparticle interactions in a problematic low-temperature region. The correct recognition of the magnetic transition process to the corresponding state is essential for further analysis and the most accurate conclusions. It also permits a plausible prediction of the effects and phenomena that are inherent to the system, although not apparent at first glance.

Yet another motivation for detailed scrutinizing of the Co/Au bimetallic NPs comes from the results of our recent works. They revealed a direct relation between super-spin-glass freezing followed by the onset of nonequilibrium magnetic dynamics and the enhanced magnetocaloric response of the NPs [20]. On the other hand, Yamamoto and co-workers [21,22] showed that, in the case of superparamagnetic systems where blocking instead of superspin freezing is dominant, magnetocaloric effect performance significantly decays with particles' size distribution increment. Further analysis of the magnetic transition in our Co/Au NPs by means of scaling laws [23] showed significant deviations of critical exponents from the values typical of mean-field theory or Ising models. In addition, the exponents do not match with those reported for nanoparticle systems where freezing of surface spins into the spin-glass state is present. Unambiguous determination of the magnetic transition nature in a nanoparticle system is, thus, crucial for fundamental understanding of its magnetocaloric response. The objective of this paper is to contribute to the elucidation of this question. The benefits of getting this kind of information will result in a better design and tuning of nanosystems.

II. EXPERIMENTAL AND MODEL DETAILS

The examined Co/Au nanoparticles are spherical and have core/shell structures. High-resolution transmission electron microscopy view of a representative particle, its scheme, and diffraction pattern of the powder sample are shown in Figs. 1(a)–1(c), respectively. The particles are composed of ferromagnetic cores of average diameter $\sim$5 nm and protective gold coatings of average thickness $\sim$1 nm.
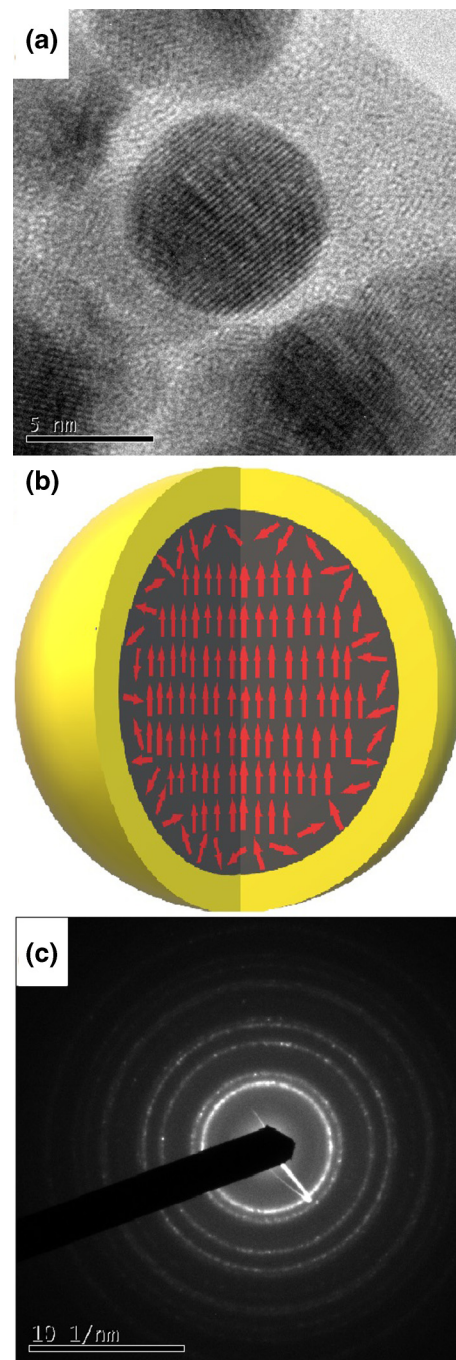

FIG. 1. (a) High-resolution TEM image of a Co/Au nanoparticle. The scheme of its core/shell structure is depicted in (b). Red arrows represent orientations of cobalt single atom spins. (c) Diffraction pattern of Co/Au powder sample.

Their size distribution is narrow. The core size is below the critical limit of ~ 50 nm reported for cobalt [24], hence, the particles are in the single-domain state. The NPs were synthesized by employing the reverse micelle method. First, pure Co cores were prepared. Then, the cores were capped by a gold layer. Details regarding utilized chemicals, process of preparation, and particles' structural and morphological analyses can be found in our previous work [25] (sample Co/Au1).

Magnetic properties of the Co/Au system were investigated utilizing a QuantumDesign superconducting quantum interference device magnetometer magnetic property measurement system 5XL. The powder sample was encapsulated into a plastic capsule and inserted into the plastic holder. Diamagnetic contribution of the capsule and holder were measured and subtracted from experimental data.

ac magnetic susceptibility was measured by applying a small oscillating driving field of amplitude $H = 2.5$ Oe superimposed on various dc fields in the range of $0 \leqslant H \leqslant 1$ kOe at frequencies of 0.1–1000 Hz.

The zero-field cooling (ZFC) and the field cooling (FC) experiments were conducted by the usual procedure. The demagnetized sample was cooled down from room temperature to 2 K in the zero magnitude of the magnetic field. Subsequently, constant magnetic-field H was applied, and magnetization (ZFC) was being recorded during the warming of the sample back to the room temperature. Afterwards, magnetic-field H stayed on, and magnetization (FC) was being measured during the cooling process back to 2 K. With the intention to examine a presence of the aging effect, the additional FC experiment ($H = 30$ Oe) was performed with the two intermittent stops at 5 and 3 K where the applied field was cut to zero for $t = 10^4$ s.

Another kind of aging experiment was conducted at conditions where the system was cooled in the ZFC protocol to the experimental temperature of 6 K. Subsequently, it was exposed to the external static magnetic field of the magnitude of 25 Oe for the period of time $t_s = 0$ and $t_s = 1000$ s. After the elapse of t_s, the magnetic field stayed on, and relaxation of magnetization was being recorded for 2 h.

For the isothermal remanent magnetization (IRM) experiment, the thermally demagnetized sample was cooled down in the ZFC protocol to the experimental temperature of 5 K. Afterwards, it was exposed to a low static magnetic field H for $t_w = 2$ s. After the elapse of t_w, the magnetic field was set to zero for a period of t_w, and the magnetic remanence $M_R(H)$ was measured, subsequently. This process was repeated with the increment of H at each step until the sample reached saturation magnetization $M_R(\infty)$.

In the case of direct current demagnetization (DCD) experiment, the demagnetized sample was cooled down in the ZFC protocol, but contrary to the IRM, a static magnetic field of high magnitude $H = 50$ kOe was applied for t_w in order to saturate the sample at the experimental temperature of 5 K. Subsequently, the static magnetic field in the direction opposite to magnetization was applied. After t_w, it was switched off, the system was kept in zero field for t_w, and, then, remanent magnetization was measured. This was repeated again, increasing the field until saturation in the opposite direction was achieved.

Evaluation of the ac susceptbility experimental data was carried out in terms of well-established theoretical models. If the interparticles' interactions are absent, critical behavior of nanoparticle superspin's relaxation time obeys the Arrhenius law [17],

$$\tau = \tau_0 \exp\left(\frac{E_a}{k_B T}\right), \tag{1}$$

where τ_0 denotes the prerelaxation constant, E_a denotes the activation energy, and k_B denotes the Boltzmann constant.

On the other hand, the occurrence of weak interactions in the system results in critical behavior described more accurately by Vogel-Fulcher law [11],

$$\tau = \tau_0 \exp\left(\frac{E^*}{k_B(T - T_0)}\right), \tag{2}$$

where E^* is the energy barrier (activation energy) modified by an effective contribution of the interparticle interactions and T_0 is the parameter corresponding to the strength of the interactions.

The dynamics of a system exhibiting strong mutual interactions among nanoparticles follows critical slowing down law in the vicinity of the magnetic transition [11],

$$\tau = \tau_0 \left(\frac{T - T_g}{T_g}\right)^{-z\nu}, \tag{3}$$

where $z\nu$ is the critical exponent and T_g is the spin-glass freezing temperature.

Further reliable analysis employing ac susceptibility data for the particles' interaction strength assessment is a frequency-dependent criterion [26],

$$p = \frac{\Delta T_{max}}{T_{max} \Delta \log_{10}(f)}, \tag{4}$$

where T_{max} denotes the average value of $\chi'(T)$ maximum temperatures in the range of experimental frequencies and ΔT_{max} is the difference between maximal and minimal values of T_{max}. The values characteristics of superspin glasses are found in interval $p \in (0.005, 0.05)$, whereas $p \in (0.1, 0.13)$ is typical of the superparamagnetic blocking process [27–29].

III. RESULTS AND DISCUSSION

A. ac experiments

A number of studies [30–32] have demonstrated that relaxation processes in the magnetic system can be reliably examined by means of ac magnetic susceptibility measurements. The analysis of $\chi(T)$ data in terms of models described in Sec. II enables to estimate the strength of interactions among particles and, subsequently, infer the behavior of nanoparticles' magnetic moments at specific conditions.

Critical slowing down [33] of super-spin-relaxation time τ with decreasing temperature close to T_{SSG} has been documented in a number of super-spin-glass systems. Suzuki *et al.* [34] and Aslibeiki *et al.* [35] investigated Fe_3O_4 nanoparticle systems by means of ac susceptibility measurements. In these studies, it was found that τ diverges at T_{SSG} obeying the power-law $\tau = \tau^*(T/T_{SSG} - 1)$. They assumed the Néel-Brown relaxation time of individual particles as the attempt
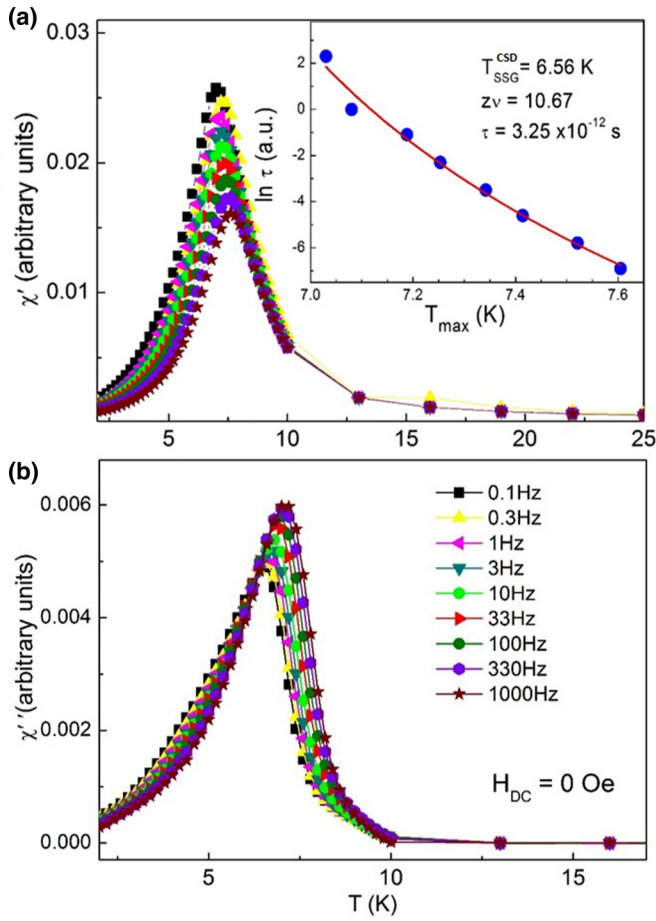
FIG. 2. (a) In-phase and (b) out-of-phase susceptibilities vs temperature dependence of the Co/Au nanoparticle system recorded in a zero dc applied field. The inset of (a) represents the fit of experimental data according to critical slowing down law.

FIG. 3. ac susceptibility data of the Co/Au system obtained at different values of dc applied magnetic fields.

time and obtained the values of $\tau^* \sim 10^{-12}$–10^{-9} s and critical exponents $zv \sim 10$ similar to spin glasses [27].

We performed the measurements of temperature variations of the in-phase (real) χ' and the out-of-phase (imaginary) χ'' parts of ac susceptibility at different frequencies and various applied dc fields. The data displayed in Figs. 2 and 3 clearly demonstrate the presence of relaxation process in the Co/Au system represented by $\chi'(T)$ and $\chi''(T)$ maxima. A significant frequency shift of $\chi'(T)$ maximum towards higher temperatures and the decrease in its value with frequency enhancement under all experimental conditions have been reported as a behavior typical of nanoparticle systems where superspin blocking or freezing occurs [36,37].

In order to determine the origin of the relaxation process, we evaluated the ac susceptibility data according to various relevant models, see our previous work [25]. Although the spin freezing temperature is often taken as the temperature at which $\chi'(T, f)$ is 0.98 times the equilibrium susceptibility for the purpose of dynamical scaling analysis, it is reasonable to define it as the temperature of maximum susceptibility in the $\chi'(T, f)$ curve as was demonstrated by Gunnarsson *et al.* [38] and Djurberg *et al.* [39]. Assuming this, we concluded that the examined Co/Au system is likely to exhibit collective
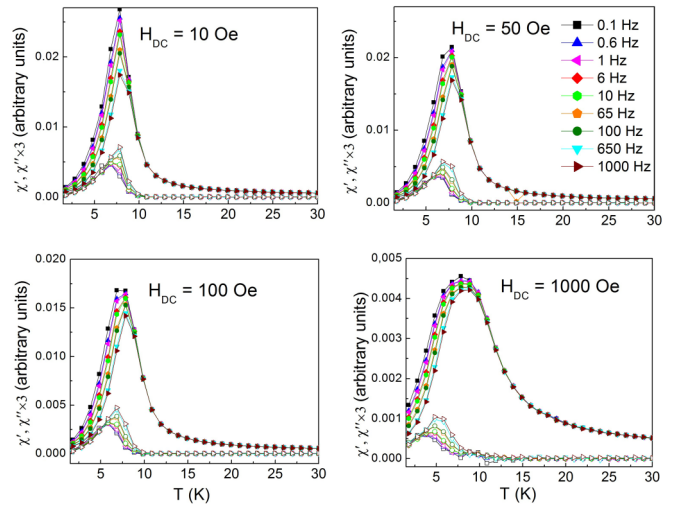
superspin freezing in spin-glass-like fashion below $T_{SSG}^{CSD} = 6.56$ K.

From the ac data fit, in terms of the critical slowing down law [the inset of Fig. 2(a)], we obtained prerelaxation constant $\tau_0 = 3.25 \times 10^{-12}$ s. The value is found in the range of 10^{-13} to 10^{-9} s that is usually reported for noninteracting magnetic nanoparticles [40]. Nevertheless, there is evidence of the τ_0 with a similar order of magnitude in the nanoparticle systems with strong interactions. Botez *et al.* [27] reported the super-spin-glass behavior in $Zn_{0.5}Ni_{0.5}Fe_2O_4$ NPs of average diameter 9 nm and $\tau_0 \sim 10^{-12}$ s. Andersson *et al.* [41] investigated the effects of the individual particle relaxation time on super-spin-glass dynamics of two dense and monodisperse γ-Fe_2O_3 nanoparticle assemblies (6 and 8 nm). They found that the microscopic relaxation time of NPs is significantly dependent on the particle size. They reported a typical value of $\tau_0 = 5 \times 10^{-9}$ s for the larger particles, whereas the value of two orders lower $\tau_0 = 2 \times 10^{-11}$ s for the smaller ones. Kesserwan *et al.* [42] studied magnetization reversal in isolated and interacting single-domain nanoparticles. Intriguingly, they concluded on a faster reversal process in the presence of the magnetic dipolar interaction. The simulation results were in good agreement with experimental measurements performed on Co/Pt core/shell nanoparticles of the sizes similar to ours. They reported the relaxation time of a particle moment $\tau_0 \sim 10^{-11}$ s at the vicinity of the transition. On the other hand, the value of the critical exponent $zv = 10.67$ obtained from the fit to our experimental data is in good accordance with the values reported for the superspin freezing process [18,27,29,40].

Another evidence for strong mutual interactions among the examined NPs discussed in Ref. [25] provided the calculation of relative variation (per frequency decade) of the in-phase susceptibility peak temperature [43]. The value $p = 0.022$ was found in the range of 0.005–0.05 that is typical of super-spin-glass systems. Also, the Cole-Cole plots exhibited the shapes of semicircles that are significantly flattened.

These findings are in accordance with two predominant features of the ac susceptibility data collected in
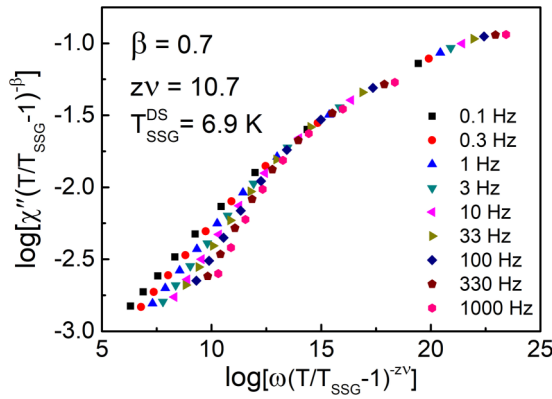
FIG. 4. Dynamic scaling of experimental $\chi''(T, f)$ data.

TABLE I. Characteristics of superspin glasses found in selected nanoparticle systems.

Nanoparticles	T_{SSG}^{CSD} (K)	$z\nu$	T_{SSG}^{DS} (K)	$z\nu$	β	T_{SSG}^{AT} (K)
Co/Au[a]	6.56	10.7	6.9	10.7	0.7	7.1
$Zn_{0.5}Ni_{0.5}Fe_2O_4$[b]	190	10	190	10	1	190
$Fe_{30}Ag_{40}W_{30}$[c]	19.7	10.2	19.7	10.2	0.8	
Fe_3O_4[d]	30.6	8.2				32.5

[a]This paper.
[b]Complex spinel ferrites of average size 9 nm [27].
[c]Highly heterogenous nanogranular system [29].
[d]Monodisperse Fe_3O_4 nanoparticles of average size 5 nm capped with organic shells [34].

various dc fields (0 to 1 kOe) presented in Figs. 2 and 3. With increasing applied field, considerable suppression and width extension of $\chi'(T)$ and $\chi''(T)$ peaks are apparent. Also, a slight upward temperature shift of $\chi'(T)$ can be recognized. Similar behaviors have been observed in conventional metallic spin glasses [44], super-spin-glass-like [$Co_{80}Fe_{20}$ (0.9-nm)/Al_2O_3 (3-nm)] multilayers [45] as well as in the Monte Carlo simulations of dynamics of reentrant Ising spin glasses [46]. When looking closely at the ac data obtained at zero applied dc field, Fig. 2, another characteristic behavior of the $\chi''(T)$ component with respect to $\chi'(T)$ can be recognized in our system. It is its sharp onset in the vicinity of $\chi'(T)$ maximum and the correspondence of its peak position with maximal gradient of $\chi'(T)$ left shoulder. The features have also been observed by de Toro *et al.* [47] in mechanically alloyed nanocrystalline Fe-Al-Cu, and they are regarded as a signature of spin-glass-like behavior.

Further confirmation of the collective superspin freezing in the Co/Au nanoparticle system was carried out by dynamic scaling analysis in the framework of critical dynamics theory [27,29,36,40]. Using the linear-response theory and the spin autocorrelation function [48], it is possible to derive the full dynamic scaling relation for the out-of-phase component of the ac susceptibility given by [29]

$$\chi''(\omega, T) = \epsilon^\beta G(\omega \epsilon^{-z\nu}), \tag{5}$$

where $\omega = 2\pi f$, β is the critical exponent defining how the order parameter approaches zero, and $\epsilon = T/T_{SSG} - 1$ is reduced temperature. Asymptotic behavior of $G(x)$ for large values of x is given by $G(x) \propto x^{\beta/z\nu}$. Employing the dynamic scaling, one can achieve data collapse of the ac susceptibility on the single curve. Figure 4 shows $\chi''(T, f)$ dependencies recorded in the zero dc applied field in scaled form according to Eq. (5). Data for the analysis have been selected from the temperature interval between the $\chi''(T, f)$ peak (6.9 K) and the temperature corresponding to ~10% of the $\chi''(T, f)$ peak value (8.6 K) [29,40]. The best collapse was obtained in the close vicinity of the peaks (temperature range of 6.9–8 K) for $T_{SSG}^{DS} = 6.9$ K, $\beta = 0.7$, and $z\nu = 10.7$. Departing from the temperature of magnetic transition T_{SSG}^{DS}, the collapse is less convincing. This is apparent in the range of low values on the ordinate (up to -2.3) that corresponds to to the temperature interval of 8–8.6 K. The extracted values of critical exponents

are in good agreement with those reported for superspin glasses [27,29,40,45]. The review of parameters characteristic of superspin glasses found in selected nanoparticle systems are listed in Table I.

Considering all the observations above, we infer the examined relaxation process is induced by freezing of Co/Au nanoparticles' superspins into the super-spin-glass state. For the unequivocal verification of this assumption and for revealing the nature of mutual inter-particle interactions, series of complementary experiments in dc fields have been performed.

B. dc experiments

The research on dc properties of superspin glasses conducted in the past two decades introduced several known signatures and well-established analysis of super-spin-glass freezing. We have examined our Co/Au nanoparticle system employing the most relevant of them, and the obtained results are discussed here.

The experiments complement previous ac studies and revealed the features typical of superspin glasses.

(i) The temperature independence of magnetization M_{FC} (recorded when cooled in the applied field) or even its decrease with lowering the temperature is usually considered as a typical super-spin-glass feature [18,36]. This behavior has been documented by Petracic *et al.* [36] in the system of fine $Co_{80}Fe_{20}$ nanoparticles embedded in a diamagnetic insulating Al_2O_3 matrix or by Hiroi *et al.* [18] in γ-Fe_2O_3/SiO_2 core-shell nanoparticles system. However, spin-glass systems with monotonous increase in M_{FC} with diminishing temperature (usually typical of superparamagnets) have also been reported [27,49]. Hence, this hallmark is challenged as an unequivocal rule for the super-spin-glass determination and additional experiments are, therefore, inevitable.

ZFC (M_{ZFC}) and FC (M_{FC}) magnetization vs temperature dependences of our Co/Au system obtained in various applied fields (5–1000 Oe) are shown in Fig. 5. M_{FC} curves obtained at lower fields (up to 100 Oe) exhibit temperature independence or tendency to saturate upon cooling towards the lowest temperatures. In the case of higher fields, the effect is not fully apparent due to the significant shift of the ZFC vs FC bifurcation point towards low temperatures. We assume the plateau could be hidden by the contribution of surface spins, see scheme in Fig. 1(b). Their contribution to the magnetization increases with decreasing temperature since
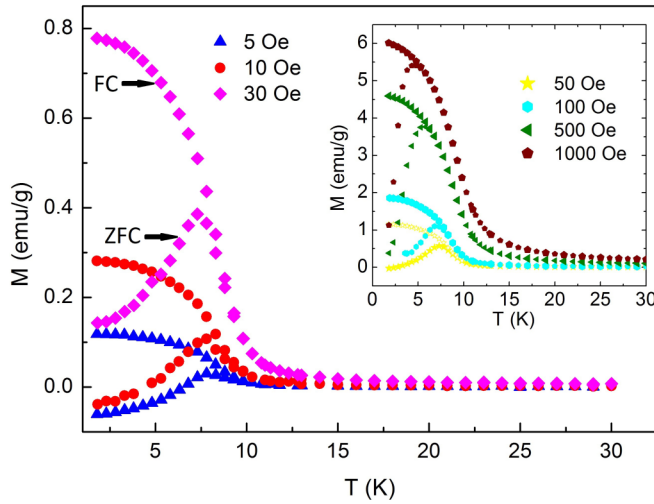
FIG. 5. Temperature variations of the ZFC and FC magnetizations of Co/Au system in different applied fields from 5 Oe to 1 kOe.

FIG. 6. The critical temperature T_g as a function of $H^{2/3}$. T_g is determined as the maximum of corresponding $d(M_{FC} - M_{ZFC})/dT$. The solid line represents the linear fit.

they continue to thermally fluctuate below T_g and freeze only at lower temperature determining the tendency to the plateau.

Although this behavior is generally ascribed to the super-spin glasses [18,27,49], it can also occur in the superparamagnetic nanoparticle systems with broad size distribution [50]. There, individual blocking, instead, of collective freezing of superspins is dominant. Since narrow M_{ZFC} maxima, Fig. 5, along with TEM and x-ray diffraction analysis, Ref. [25], clearly point to low dispersion of nanoparticle sizes in the Co/Au system, we infer that low-temperature M_{FC} flatness is likely the hallmark of the super-spin-glass state.

(ii) Another strong evidence suggesting the presence of low-temperature super-spin-glass phase in our Co/Au system comes from the critical temperature dependence on external dc magnetic-field $T_g(H)$. In superparamagnetic NPs, different approaches are commonly used for blocking temperature determination from ZFC-FC data. Bruvera *et al.* [51] and Micha *et al.* [52] showed that the most appropriate one is the method based on the T derivative of the difference between ZFC and FC curves. Although the technique assumes noninteracting NPs, we adopted this approach and determined the corresponding $T_g(H)$ values as the maxima of $d(M_{FC} - M_{ZFC})/dT$. In our system, the extracted T_g values exhibit a linear decrease with $H^{2/3}$, Fig. 6, following the de Almeida-Thouless line (AT line) expressed as [53]

$$H \propto \left[1 - T_g(H)/T_{SSG}^{AT}\right]^{3/2}, \qquad (6)$$

where H is the applied dc field and T_{SSG}^{AT} is the super-spin-glass freezing temperature. The intercept of the temperature axis and the AT line yields the value of zero-field freezing temperature. The value of $T_{SSG}^{AT} = 7.1$ K determined for the examined Co/Au system is in good agreement with the value extracted from full dynamic scaling of ac data. Nevertheless, a slight dispersion of the super-spin-glass freezing temperature T_{SSG} is apparent in the system, see Table I. The deviations can be ascribed to the several reasons. Despite rather narrow size distribution, the investigated Co/Au NPs cannot be regarded as monodisperse. Due to this, there is a distribution in the
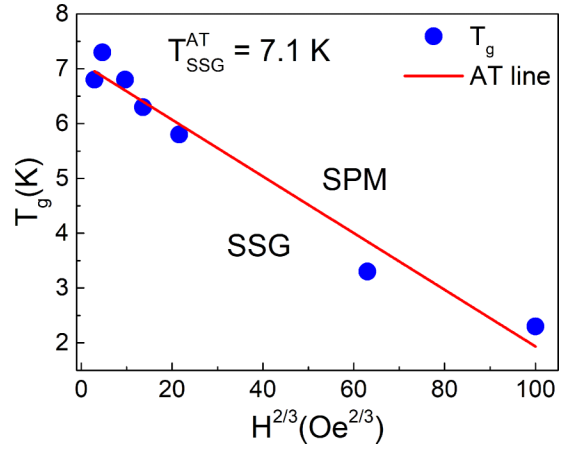
particles' relaxation times, magnetic moments, and mutual distances. The system has been examined in the conditions with the vast parameters' variations (order of four). All the analyses have been performed on the different experimental datasets. Taking into account the limitations and fundamental peculiarities inherent to each of the applied methods, slight discrepancies in the results can be expected.

(iii) The occurrence of nonequilibrium dynamics manifested by typical magnetic relaxation and the aging effect is another signature attributed to supers pin glasses as a representative of systems with a broad distribution of magnetic moment relaxation time [36]. Peddis *et al.* [54] and De Toro *et al.* [55] clearly demonstrated the presence of these phenomena in $MnFe_2O_4$ nanopowders and dense maghemite nanoparticle systems, respectively, in the temperature region below 10 K. Figure 7 shows magnetization relaxation data of our Co/Au system obtained at $T = 6$ K where we supposed
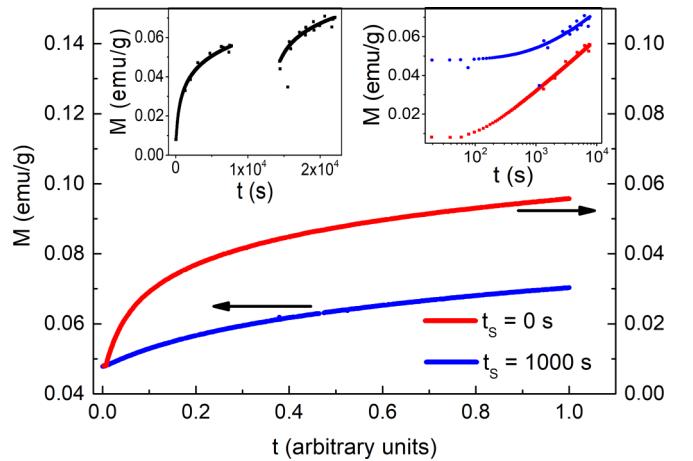

FIG. 7. Relaxation of the magnetization collected in 25-Oe applied dc field after the exposition of the system to the external magnetic field for $t_s = 0$ and $t_s = 1000$ s. The timescale was normalized with respect to the duration of the magnetization recording. The insets show experimental data plotted on linear and logarithmic timescales.
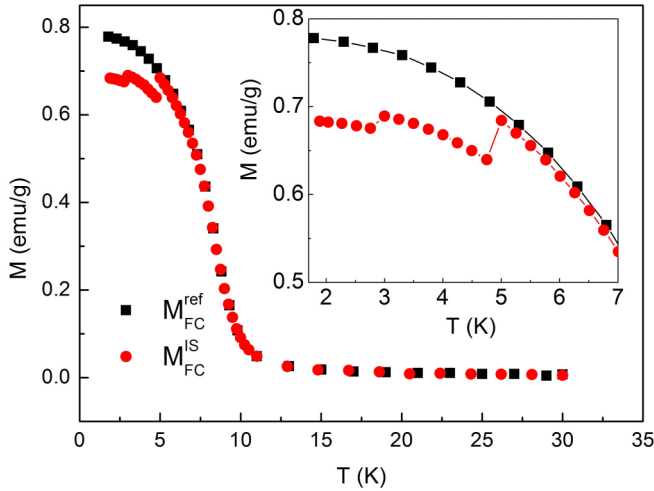
FIG. 8. FC magnetization vs temperature (M_{FC}^{ref}) obtained in the applied field of 30 Oe and FC magnetization vs temperature data recorded with intermittent stops (M_{FC}^{IS}) at $T = 5$ and $T = 3$ K where the field was cut for a period of $t = 10^4$ s.

FIG. 9. Henkel plot of the Co/Au system constructed from the experimental data obtained at the temperature of 5 K.

the nanoparticles' superspins are frozen. As is apparent, relaxation of magnetization after exposing the system to magnetic field for 1000 s differs significantly from the case of 0-s exposure. In contrast, if the superspins of the particles were blocked (equilibrium state), both curves should overlap because the same characteristic is being measured, although at different times. The effect observed in our experiment exhibit characteristics similar to the aging effect that is typical of nonequilibrium dynamics characteristic of super-spin-glass systems [56,57]. Furthermore, the relaxation of magnetization in an applied field of low magnitude exhibits linear dependence when plotted vs $\log_{10}(t)$, Fig. 7 (inset) [58]. The slow glassy dynamics is another hallmark of a wide energy barrier distribution in our system. It can occur as the consequence of particles polydispersity and/or the presence of interparticle interactions [59].

Figure 8 shows M_{FC}^{IS}, that denotes FC magnetization ($H = 30$ Oe) recorded with intermittent stops ($H = 0$ Oe) at $T = 3$ and $T = 5$ K (details of the measurement are described in Sec. II), compared with M_{FC}^{ref} obtained by standard FC protocol. Although the steplike character of M_{FC}^{IS} of investigated, the Co/Au system is the feature recognized in superspin glasses [34,60], Zheng et al. [61] and Sasaki et al. [50] demonstrated that this behavior may also exhibit typical superparamagnets. Therefore, the presence of the super-spin-glass state in the Co/Au NPs is necessary to verify by means of other methods.

It is commonly accepted that the Henkel plot is a tool to analyze the character and the strength of interactions in the magnetic particle system [62,63]. It is constructed as a dependence of normalized values of the direct current demagnetization $m^{DCD} = M^{DCD}(H)/M_S^{DCD}$ vs the isothermal remanent magnetization $m^{IRM} = M^{IRM}(H)/M_S^{IRM}$, Fig. 9. M_S^{IRM} and M_S^{DCD} are the values of corresponding saturation magnetization. According to the Stoner-Wolfarth model [12,64] designed for the noninteracting nanoparticle system, the m^{DCD} vs m^{IRM} dependence should obey the Wolfarth equation [64],

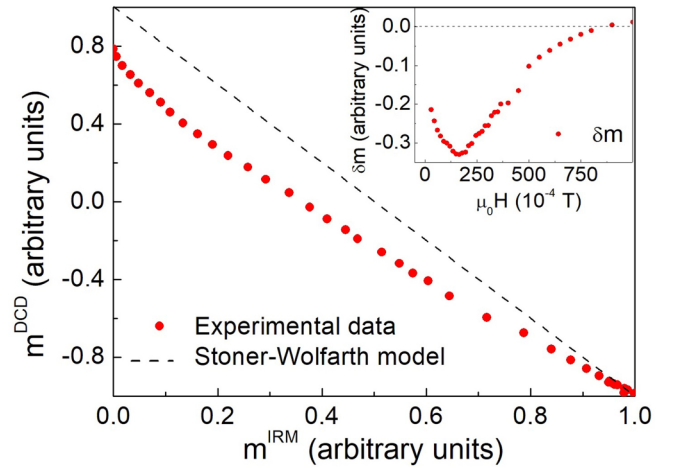$$m^{DCD}(H) = 1 - 2m^{IRM}(H), \qquad (7)$$

that results in the straight diagonal (dashed) line in the Henkel plot, Fig. 9. If the experimental data are found in the region below the Wolfarth line, (negative) interactions that aid a demagnetized state dominate in the system. On the other hand, the presence of the experimental data above the Wolfarth line signifies the prevalence of (positive) interactions promoting the magnetized state [62,63]. Figure 9 clearly demonstrates the predominance of negative interactions in the Co/Au system at $T = 5$ K. García-Otero et al. [62] carried out Monte Carlo simulations of interactions among single-domain ferromagnetic particles. They reported that noninteracting particles with cubic anisotropy always show positive deviation of the Henkel plot. However, due to the presence of dipolar (negative) magnetic interactions in the system, the deviation changes gradually from positive to negative with increasing strength of the interaction. Since fine Co particles (magnetic cores of our Co/Au NPs) crystallize in the cubic ϵ-cobalt phase, see Ref. [25], and strong magnetic dipole-dipole interactions are characteristic of superspin glasses, we assume that investigated Co/Au system is in the SSG state at $T = 5$ K.

IV. CONCLUSION

The bimetallic Co/Au nanoparticle system has been profoundly studied with the aim to unambiguously discriminate the origin of the magnetic transition occurring at $T \sim 7$ K. Application of selected well-established methods provided a wealth of complementary information about the character of investigated transition and brought up consistent results. The presence of strong dipolar interparticle interactions is clearly evidenced by the Henkel plot. Critical slowing down of the relaxation, dynamic scaling of $\chi''(T, f)$ data, and aging effects are observed. All of these features are inextricably connected to collective freezing, instead, of superparamagnetic blocking of particles' magnetic moments. Assuming all the results, we concluded that superspins of individual Co/Au nanoparticles under the influence of strong dipole-dipole magnetic interactions below T_{SSG} exhibit collective behavior and freeze into the super-spin-glass state.

[1] A. Singh and S. K. Sahoo, Drug Discov. Today **19**, 474 (2014).

[2] O. C. Farokhzad, Nature (London) **526**, 47 (2015).

[3] C. Li, J. Ciston, and M. Kanan, Nature (London) **508**, 504 (2014).

[4] D. Fiorani, in *Surface Effects in Magnetic Nanoparticles* (Springer-Verlag, New York, 2005), p. 300.

[5] D. Peddis, M. Mansilla, S. Mørup, C. Cannas, A. Musinu, G. Piccaluga, F. D'Orazio, F. Lucari, and D. Fiorani, J. Phys. Chem. B **112**, 8507 (2008).

[6] T. Shendruk, R. Desautels, B. Southern, and J. Van Lierop, Nanotechnology **18**, 455704 (2007).

[7] M. P. Morales, S. V. Verdangure, M. I. Montero, C. J. Serna, A. Roig, L. Casas, B. Martinez, and F. Sandiumenge, Chem. Mater. **11**, 3058 (1999).

[8] H. Khurshid, P. Lampen-Kelley, Ò. Iglesias, J. Alonso, M. H. Phan, C. J. Sun, M. L. Saboungi, and H. Srikanth, Sci. Rep. **5**, 1 (2015).

[9] E. Winkler, R. Zysler, M. Mansilla, D. Fiorani, D. Rinaldi, M. Vasilakaki, and K. Trohidou, Nanotechnology **19**, 185702 (2008).

[10] T. Zhu, B. Shen, J. Sun, H. Zhao, and W. Zhan, Appl. Phys. Lett. **78**, 3863 (2001).

[11] O. Petracic, Superlatt. Microstruct. **47**, 569 (2010).

[12] E. C. Stoner and E. P. Wohlfarth, Philos. Trans. Roy. Soc. A **240**, 599 (1948).

[13] L. Néel, Ann. Geophy. **5**, 99 (1949).

[14] B. Aslibeiki, P. Kameli, H. Salamati, M. Eshraghi, and T. Tahmasebi, J. Magn. Magn. Mater. **322**, 2929 (2010).

[15] D. Parker, V. Dupuis, F. Ladieu, J.-P. Bouchaud, E. Dubois, R. Perzynski, and E. Vincent, Phys. Rev. B **77**, 104428 (2008).

[16] X. Chen, S. Bedanta, O. Petracic, W. Kleemann, S. Sahoo, S. Cardoso, and P. P. Freitas, Phys. Rev. B **72**, 214436 (2005).

[17] S. Mørup, M. Hansen, and C. Frandsen, Beilst. J. Nanotechnol. **1**, 182 (2010).

[18] K. Hiroi, K. Komatsu, and T. Sato, Phys. Rev. B **83**, 224423 (2011).

[19] F. Hellman, D. R. Queen, R. M. Potok, and B. L. Zink, Phys. Rev. Lett. **84**, 5411 (2000).

[20] O. Kapusta, A. Zeleňáková, P. Hrubovčák, R. Tarasenko, and V. Zeleňák, Int. J. Refrig. **86**, 107 (2018).

[21] T. Yamamoto, M. Tanaka, Y. Misaka, T. Nakagawa, T. Nakayama, K. Niihara, and T. Numazawa, Scr. Mater. **46**, 89 (2002).

[22] T. Kinoshita, S. Seino, H. Maruyama, Y. Otome, K. Okitsu, T. Nakayama, K. Niihara, T. Nakagawa, and T. Yamamoto, J. Alloys Compd. **365**, 281 (2004).

[23] A. Zeleňáková, P. Hrubovčák, V. Zeleňák, J. Kováč, and V. Franco, J. Alloys Compd. **805**, 767 (2019).

[24] M. Sato and Y. Ishii, J. Appl. Phys. **54**, 1018 (1983).

[25] P. Hrubovčák, A. Zeleňáková, V. Zeleňák, and J. Kováč, J. Alloys Compd. **649**, 104 (2015).

[26] M. Tadić, V. Kusigerski, D. Marković, I. Milosević, and V. Spasojević, J. Magn. Magn. Mater. **321**, 12 (2009).

[27] C. E. Botez, A. H. Adair, and R. J. Tackett, J. Phys.: Condens. Matter **27**, 76005 (2015).

[28] J. De Toro, S. S. Lee, D. Salazar, J. L. Cheong, P. Normile, P. Muñiz, J. Riveiro, M. Hillenkamp, F. Tournus, A. Tamion, and P. Nordblad, Appl. Phys. Lett. **102**, 183104 (2013).

[29] J. A. De Toro, M. A. López de la Torre, J. M. Riveiro, A. Beesley, J. P. Goff, and M. F. Thomas, Phys. Rev. B **69**, 224407 (2004).

[30] M. Bałanda, Acta Phys. Pol. A **124**, 964 (2013).

[31] C. V. Topping and S. J. Blundell, J. Phys.: Condens. Matter **31**, 013001 (2019).

[32] F. Bensebaa, in *Nanoparticle Technologies*, edited by F. Bensebaa, Interface Science and Technology Vol. 19 (Elsevier, Cambridge, MA, USA, 2013), pp. 385–427.

[33] A. T. Ogielski, Phys. Rev. B **32**, 7384 (1985).

[34] M. Suzuki, S. I. Fullem, I. S. Suzuki, L. Wang, and C.-J. Zhong, Phys. Rev. B **79**, 024418 (2009).

[35] B. Aslibeiki, P. Kameli, I. Manouchehri, and H. Salamati, Current Appl. Phys. **12**, 812 (2011).

[36] O. Petracic, X. Chen, S. Bedanta, W. Kleemann, S. Sahoo, S. Cardoso, and P. Freitas, J. Magn. Magn. Mater., **300**, 192 (2006).

[37] S. Bedanta and W. Kleemann, J. Phys. D: Appl. Phys. **42**, 013001 (2008).

[38] K. Gunnarsson, P. Svedlindh, J.-O. Andersson, P. Nordblad, L. Lundgren, H. Aruga Katori, and A. Ito, Phys. Rev. B **46**, 8227 (1992).

[39] C. Djurberg, P. Svedlindh, P. Nordblad, M. Hansen, F. Bødker, and S. Mørup, Phys. Rev. Lett. **79**, 5154 (1997).

[40] F. H. Aragón, P. E. De Souza, J. A. Coaquira, P. Hidalgo, and D. Gouvêa, Physica B **407**, 2601 (2012).

[41] M. S. Andersson, J. A. De Toro, S. S. Lee, P. S. Normile, P. Nordblad, and R. Mathieu, Phys. Rev. B **93**, 054407 (2016).

[42] H. Kesserwan, G. Manfredi, J.-Y. Bigot, and P.-A. Hervieux, Phys. Rev. B **84**, 172407 (2011).

[43] M. Tadić, D. Marković, V. Spasojević, V. Kusigerski, M. Remškar, J. Pirnat, and Z. Jagličić, J. Alloys Compd. **441**, 291 (2007).

[44] V. Cannella and J. A. Mydosh, Phys. Rev. B **6**, 4220 (1972).

[45] S. Sahoo, O. Petracic, C. Binek, W. Kleemann, J. B. Sousa, S. Cardoso, and P. P. Freitas, Phys. Rev. B **65**, 134406 (2002).

[46] J. O. Andersson, T. Jonsson, and J. Mattsson, Phys. Rev. B **54**, 9912 (1996).

[47] J. A. De Toro, M. A. López de la Torre, J. M. Riveiro, R. Sáez Puche, A. Gómez-Herrero, and L. C. Otero-Díaz, Phys. Rev. B **60**, 12918 (1999).

[48] P. Nordblad and P. Svedlindh, in *Spin Glasses and Random Fields*, edited by A. P. Young (World Scientific, Singapore, 1998).

[49] K. Vijayanandhini, C. Simon, V. Pralong, V. Caignaert, and B. Raveau, Phys. Rev. B **79**, 224407 (2009).

[50] M. Sasaki, P. E. Jönsson, H. Takayama, and H. Mamiya, Phys. Rev. B **71**, 104405 (2005).

[51] I. J. Bruvera, P. Mendoza Zélis, M. Pilar Calatayud, G. F. Goya, and F. H. Sánchez, J. Appl. Phys. **118**, 184304 (2015).

[52] J. S. Micha, B. Dieny, J. R. Régnard, J. F. Jacquot, and J. Sort, J. Magn. Magn. Mater. **272-276**, 2003 (2004).

[53] J. R. L. de Almeida and D. J. Thouless, J. Phys. A **11**, 983 (1978).

[54] D. Peddis, M. Vasilakaki, K. Trohidou, and D. Fiorani, Magnetics, IEEE Trans. Magn. **50**, 1 (2014).

[55] J. A. De Toro, S. S. Lee, R. Mathieu, P. S. Normile, D. Salazar, J. L. Cheong, P. Muniz, J. M. Riveiro, M. Hillenkamp, A. Tamion, F. Tournus, and P. Nordblad, J. Phys.: Conf. Ser. **521**, 012011 (2014).

[56] S. Sahoo, O. Petracic, C. Binek, W. Kleemann, J. B. Sousa, S. Cardoso, and P. P. Freitas, J. Phys.: Condens. Matter **14**, 6729 (2002).

[57] D.. Peddis, M. Hudl, C. Binns, D. Fiorani, and P. Nordblad, J. Phys.: Conf. Ser. **200**, 072074 (2010).

[58] R. W. Chantrell, A. Lyberatos, and E. P. Wohlfarth, J. Phys. F **16**, 6 (1986).

[59] V. Dupuis, F. Bert, J. P. Bouchaud, J. Hammann, F. Ladieu, D. Parker, and E. Vincent, Pramana **64**, 1109 (2005).

[60] Y. Sun, M. B. Salamon, K. Garnier, and R. S. Averback, Phys. Rev. Lett. **91**, 167206 (2003).

[61] R. K. Zheng, H. Gu, and X. X. Zhang, Phys. Rev. Lett. **93**, 139702 (2004).

[62] J. García-Otero, M. Porto, and J. Rivas, J. Appl. Phys. **87**, 7376 (2000).

[63] J. Lintelo and J. Lodder, J. Appl. Phys. **77**, 6416 (1995).

[64] E. Wohlfarth, J. Appl. Phys. **29**, 595 (1958).